VIDYASAGAR UNIVERSITY

Dept. of Geography

Estimation of Relationships Between Land Surface Temperature and Land Use Diversity in the Contai Municipality Area, West Bengal

*[1]Dipankar Mondal,[2]Mrinmay Mandal, [3]Subrata Jana and [4]Ashis Kumar Paul

[1,2,4]Department of Geography, Vidyasagar University, Midnapore, West Bengal, India
[3]Department of Geography, Belda College, Belda, West Bengal, India

ABSTRACT

The variation of land surface temperature (LST) in the urban area is depending on the land use and land cover (LULC) pattern. In a recent period, the changing LULC pattern is creating a harsh impact on the urban environment by increasing temperature with the built-up area development. The contradictory pattern of LST has been observed in the built-up and vegetation-covered surfaces within an urban area. The urban morphology is also an important determinant of LST variation. The purpose of the present investigation is to find out the relationships between LST patterns and land use diversity of Contai municipality area. The LULC pattern and LST have been estimated based on the Landsat 8 (OLI/TIRS) satellite data of 2018. The resultant data sets have been further correlated to estimate the impact of escalating built-up areas and vegetation cover on LST variation. The correlation shows that with the increasing built-up density the LST has been increasing (0.11), whereas, it is reverse with the vegetation density (-0.13). The municipality town of Contai should maintain buffer areas of vegetation cover surface to reduce or to stabilize the increasing LST pattern at present.

Introduction:

More than 61% of the global population is predicted to live in the urban areas by 2030 (DESA, 2012), moreover, about 40% of the world's population already exists within the 100 km of the low elevated coastal areas of East Asia &the Pacific (Barbier, 2015). However, most of the coastal areas become liable to vulnerability and are not suitable for the establishment of settlements (De Sherbininet al., 2007; McGranahan et al., 2007; Adelekan, 2010). Therefore, people choose the most suitable position in the coastal areas to build their settlements. Mostly, the coastal peoples preferred the dune ridges and more elevated natural levees for their living place rather than the other coastal landforms (Nordstrom, 2004). The elevated and undulated dune ridge tops have been degraded and flattened for preparing a more suitable place to build a settlement (Nordstrom, 2004). Moreover, people are compelled to establish their settlements in a compact way within the elongated dune ridges, as the low-lying areas of the chenier surface have been utilized for agricultural activities. The natural dune vegetations have been gradually degraded due to the increasing rate of land requirements for settlement construction (Wu & Ci, 2002). Therefore, a contrast situation is arising within the dune landscape through a dramatic reduction of green space and the same proportion increases of concrete structures in the form of urbanization (Naveh& Lieberman, 2013).

The urban morphological structure insists on forming an urban heat island (UHI) phenomenon and thermal environment (Ahmed et al., 2014). The spatio-temporal variation of land surface temperature (LST) in urban areas depends on the land use and land cover (LULC) pattern (Gartland, 2008; Emmanuel, 2005). The LULC pattern controls the rate of evaporation, albedo and

Correspondence to Dipankar Mondal
Department of Geography, Vidyasagar University, Midnapore, West Bengal, India
E-mail address : dipankargeo@gmail.com

solar radiation. These factors determine the LST distribution within an urban area. Several studies stress the built-up structure and vegetation covers have a pivotal control in heat disparities and associated LST variations in an urban area (Oke, 2002; Taha, 1997; Chudnovsky et al., 2004; Prado & Ferreira, 2005; Santamouris, 2007; Yang & Li, 2009; Kantzioura et al., 2012). The proportional distribution of open space, street orientation, green space and built-up structure is not concerned in unplanned cities. Therefore, the UHI effects have been greater apprehensive in unplanned urban areas rather than planned cities.

The present study has been carried out over the Contai municipality town which is an unplanned town concerning the urban planning approach. The urban morphology emphasizes that the city maintains very poor planning in concern of heat distribution and urban comfort. This town exists in the coastal area mainly over the dune where maximum settlement has grown up over the dune and beside the road network line. The existing open space is composed of sand and deforested areas are continuously flown from the natural dune landscape. Housing rules and customs on behalf of the environment act the health of the urban ecosystem did not maintain at the time of built-up construction.

The present study investigates the relationship between land use density (built-up area and vegetation) and temperature distribution throughout the study area. The prime objective is to search the relation (positive or negative) between temperature and vegetation cover density and similarly in case of built-up area density in Contai municipality.

2. Literature review

LULC change and effects of UHI in the urban areas are now an emerging issue in the global climate change scenario (Sahana et al., 2019). Such kind of studies has been carried out mainly in the major populous cities in the tropical areas as well as in the world (Farina, 2012; Hokaoet al., 2012; Mohan et al., 2012; Grover& Singh, 2015; Kikon et al., 2016; Wang et al., 2016). Also, very little concentration has been given in the municipality towns in the Indian perspectives (Pal& Ziaul, 2017; Ziaul& Pal, 2018; Das& Das, 2020; Ziaul& Pal, 2020). Moreover, in the global climate change and SLR situation, the coastal areas are prone to more vulnerable, and the coastal towns will be faced with harsh impacts shortly. The tremendous population pressure over the coastal land will create the escalating landscape dynamism to provide a potential level of

resource and suitable land for settlement areas (Baechler, 1998; Raleigh&Urdal, 2007; Lambin&Meyfroidt, 2011). The process and degree of land use transformation in the core area and its periphery is an important aspect to understand the future urban growth and the related impact of UHI (Shi et al., 2012).

The satellite image base LULC classification is now productive ways of finding out the land use dynamism. Depending on the image type and resolution, the enhanced level of LULC products has come out through which the land use dynamism easily can analyse (Li &Yeh, 2004; Deng et al., 2008; Chander et al., 2009; Markham et al., 2014; NASA, 2016; Bouaziz et al., 2017). The LST is also estimated from the satellite images (Yuan& Bauer, 2007; Rajeshwari& Mani, 2014; Wang et al., 2015) with the land use patterns in the urban areas.

3. Study area

In 1958 the Contai town was established as a municipal corporation in Purba Medinipur District, West Bengal at about 10 km landward position of the present-day shoreline of the Bay of Bengal (Fig. 1). Initially, this town was set up over the dune ridge which is expanded in the eastern and western side of the dune ridge also in the low-lying swale landscape of the chenier surfaces (Paul, 2002). The average elevation of the dune ridge surface is about 11.5 m, whereas, the chenier surface belongs to 6 m. Geologically, the sand dune was formed during the Late Holocene period as recent dune formation with the composition of medium-grained sand (Jana & Paul, 2018). The low-lying swale surface was formed during the Middle Holocene period as Panskura formation with the composition of the fine sand, silt and clay materials. In the geomorphological perspective, the entire area has been situated with the dune landscape (east-west), ancient tidal depositional surface (in the north of dune ridge) and Holocene tidal depositional surface (in the south of dune ridge). Since establishment, the administrative boundary and the number of wards have been increased temporally like 14 (in 1991), 18 (in 2001), 20 (in 2011) and 21 (in 2018). As per 2018, the study area exists with 14.35 km² geographical area (Fig. 1). The total population of the municipality area is 92226 (2011census). However, the main town has been covered within the wards of 9, 10, 11, 13 and 15, 16, 17 and 19 with a total population of 36931 (2011 census). The market and retailing along with cashew nut processing based economic prosperities bringing the high rate of a concretization in a concentrated pattern in the main urban centre and its surroundings.

Becoming a coastal town, Contai is fair, being neither hot nor too cold. The highest mean monthly temperature is found in summer i.e. 34° C in April to May and the temperature goes down in winter 19° C. This town and its surrounding area face about 5 – 6 cyclonic activities in a year due to the nearer location of Bay of Bengal(Singh et al., 2001). The major portion of the land area has been covered by agricultural land, settlement and sand-dunes. This town has great importance on behalf of the tourism and commercial trading in southern West Bengal (Das et al., 2013).

4. Materials and methods

4.1. LULC classification

The objective of this study is to clarify the relation between LST distribution and land use density in the Contai urban area. To assess this relationship, the Landsat 8 (OLI/TIRS) satellite image of 27 January 2018

has been classified through ENVI 5.2 software. Before classification, the Fast Line-of-sight Atmospheric Analysis of Hypercubes (FLAASH) atmospheric correction has also been done after the radiometric corrections (ENVI, 2009). The FLAASH model is used to remove or minimize the influence of atmospheric noise from the object reflectance. The radiometric correction of the OLI sensor has been done on the satellite image of Landsat 8. In this process, the Digital Numbers (DNs) have been converted to radiance value for the Landsat 8 image using the Eq. 1.1 (Chander et al., 2009; Markham et al., 2014; Mishra et al., 2014).

$$L_\lambda = (M_L \times Q_{cal}) + A_L \ \dots\dots\dots\dots (1.1)$$

where L_λ is the spectral radiance, M_L is the radiance multiplicative scaling factor for the band, A_L is the radiance additive scaling factor for the band, and Q_{cal} is the pixel value in DN of the level 1 (L1) product image.
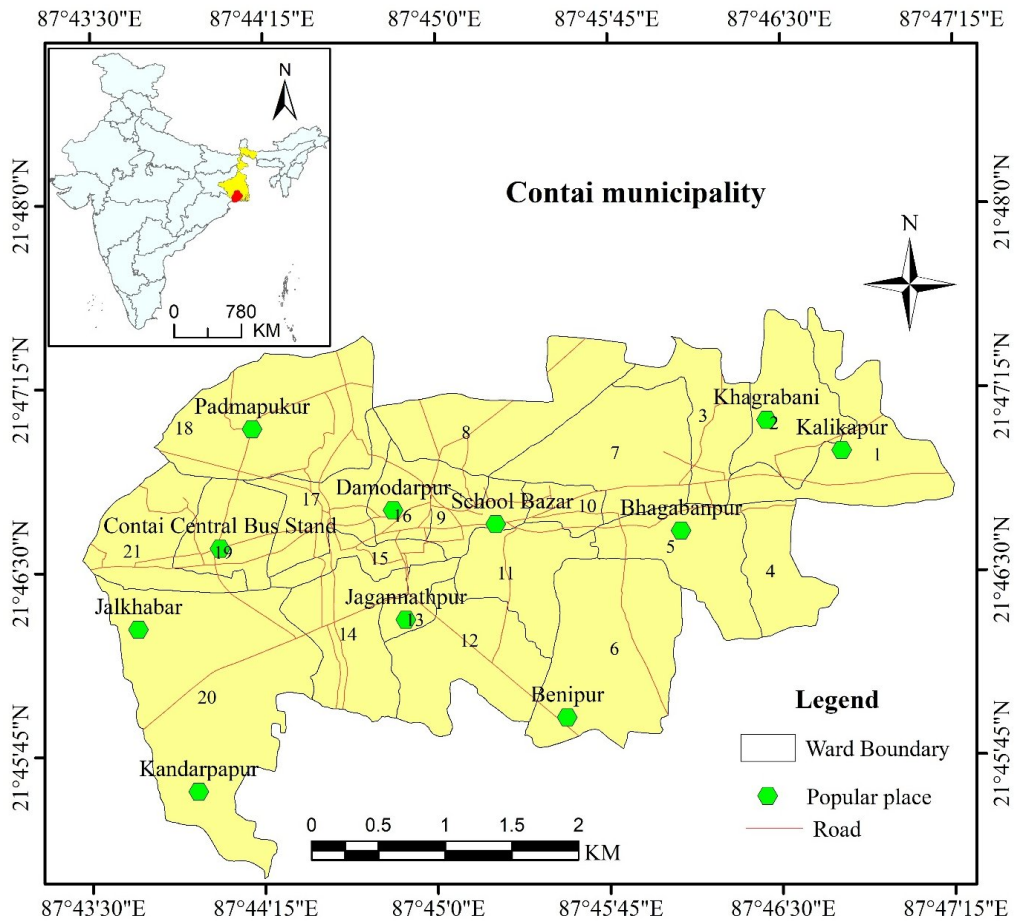

Fig. 1 : Location map of the Contai municipality area

Reflectance rescaling coefficient factor is used to convert the Top of Atmospheric (TOA) planetary reflectance of multispectral bands of the satellite data. The Eq. 1.2 is considered to switch the spectral radiance to TOA reflectance for Landsat data (NASA, 2016).

$$\rho_p = \frac{(\pi \times L_\lambda \times d^2)}{(ESUN_\lambda \times \cos\theta_s)} \quad .... (1.2)$$

where, ρ_p is the unit less planetary reflectance, which is the ratio of reflected versus total power of energy (NASA, 2016); L_λ is the spectral radiance at the sensor's aperture (at satellite radiance); d is the earth-sun distance in astronomical units (provided with Landsat 8 metadata file; $ESUN_\lambda$ is the mean solar exo-atmospheric irradiances; θ_s is the solar zenith angle in degrees, which is equal to $(\theta_s = 90° - \theta_e)$, where θ_e is the sun elevation; $ESUN$ is the $(\pi \times d^2) \times$ radiance maximum and reflectance maximum.

So, the Landsat 8 images are made available with band-specific rescaling factors which allow for the straight conversion from Digital Number (DN) to TOA reflectance. On the other hand, the property of the atmosphere (i.e. Disturbance on the reflectance that varies with the wavelength) should be considered to calculate the reflectance at the surface (Eq. 1.3), which is described by the land surface reflectance (ρ) (Moran et al., 1992).

$$\rho = \frac{\{\pi \times (L_\lambda - L_p) \times d^2\}}{[T_v \times \{(ESUN_\lambda \times \cos\theta_s \times T_z\} + E_{down}]} \quad .... (1.3)$$

where L_p is the path radiance; T_v is the atmospheric transmittance in the viewing direction; T_z is the atmospheric transmittance in the illumination direction; E_{down} is the down welling diffuse irradiance.

The supervised classification techniques, Spectral Angle Mapping (SAM) and Support Vector Machine (SVM) algorithm are applied in the Landsat image of 2018 of the selected area for the LULC classification (Pal & Mather, 2004, 2005; Bouaziz et al., 2017). In this study, based on the spatial coverage of the study areas, about 15 points of each class were demarcated depending on the on-field knowledge for the LULC classification. Based on the requirement the five LULC classes have been extracted. The classified images (2018) were further validated with the field verification, and the LULC classification was finally considered for this study when the classification was more than 89 percent accurate based on the Kappa coefficient (Smits et al., 1999). Moreover, year to year LULC conversions has been estimated using a conversion matrix (Li &Yeh, 2004; Deng et al., 2008).

4.2. Density estimation

The settlement and vegetation density have been estimated of the entire study area after dividing the
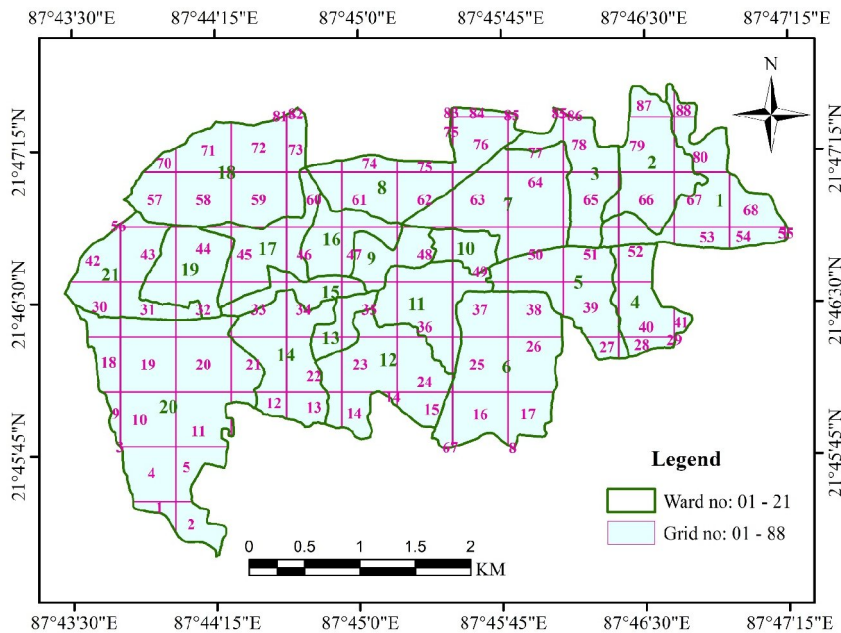

Fig. 2 : Grid map of Contai municipality area with ward and grid numbers.

entire municipality area into 88 grids adopting the Fishnet tool in ArcGIS 10.4 software (Fig. 2). Every grid area is 0.25 km² except the grids of the fringe areas of the municipality. These grids have been overlapped with the LULC and intersect to get individual grid information i.e. the amount and density of targeted land use. The settlement (SD) and vegetation (VD) density information are calculated by Eq. 1.4 and 1.5, respectively.

$$SD = \frac{S_{ag}}{A_g} \ .... \ (1.4)$$

$$VD = \frac{V_{ag}}{A_g} \ .... \ (1.5)$$

where the area under settlement (S_{ag}) and vegetation (V_{ag}) with a grid area (A_g).

4.3. LST estimation

The grid-wise LST has been estimated from the Landsat 8 (TIRS) satellite data of 27 January and 19 May 2018 using the mono window algorithm in ERDAS Imagine 14 software (Wang et al., 2015). Grid-wise temperature information is collected from the selected two images for winter (27 January 2018) and summer (19 May 2018) seasons.

The estimated grid-wise results of the settlement and vegetation density and temperature distribution the respective maps are prepared through the kernel density method in ArcGIS 10.4 software.

5. Results and discussions

5.1 LULC type

LULC is the most important factor for the variation of the LST. Particularly in the urban areas, it has a significant impact on the local level diversity of the LST. In the Contai municipality area, the LULC classification of 2018 reveals the five major LULC classes (Fig. 3). The vegetation cover is significantly higher in the eastern side over the sand dune and in the fringe areas of the sand dunes. The settlement areas have been concentrated in the central part as well as in the middle portion of the dune ridge. However, the settlement areas have been extended in the low-lying parts of the study area. The vacant areas have also been sparsely distributed in the dune ridges. The agricultural land has been extended in the eastern and western side of the sand dune in the low-lying areas. The water bodies have been mainly located in the dune fringe areas. The areal coverage of the different LULC parameters has been shown in Table 1, which indicates the dominance of agricultural land (6.60 km²) and vegetation cover (4.90 km²). However, the settlement area has been low (2.21 km²) in comparison to the vegetation and agricultural land area, but it has a great impact on the LST variation in the dune belt.
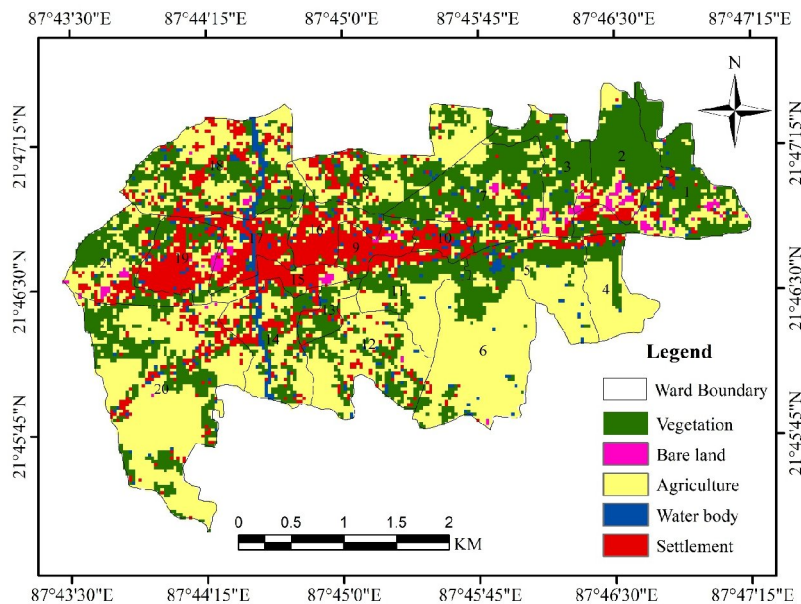

Fig. 3 : LULC types of the Contai municipality area during 2018.

Table 1. Land use and land cover types in Contai in 2018.

LULC type	Area (km^2)
Vegetation	4.90
Bare land	0.17
Agricultural land	6.60
Water	0.46
Built-up/Settlement	2.21

5.2. Built-up density

The result shows that highly dense (0.75/km²) built-up areas remained within the ward number of 9, 15, 16, 17 and 19. Whereas, the lowest density (0.03/km²) found in the fringe areas of ward number 1, 2, 20, 6 and 12 (Fig. 4). High dense built-up areas are concentrated around the Central Bus Stand located in ward 19 and Supper Market area located in ward 9 and 15. The low density is found in the dune margin and far fringe areas of the municipality.
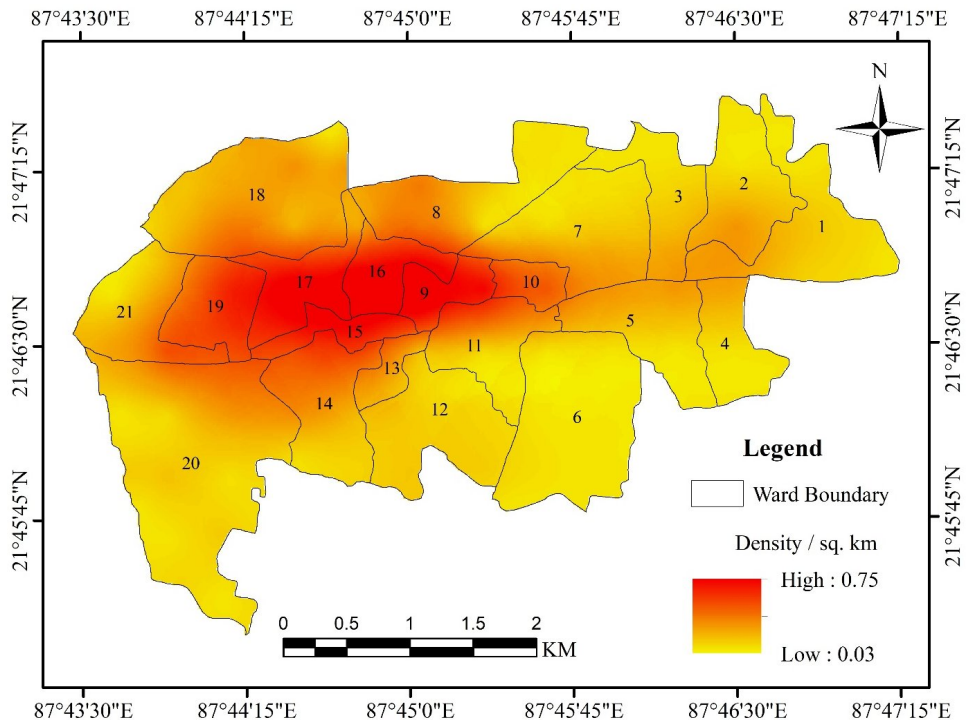
5.3. Vegetation density

The density of vegetation covers shows a reverse scenario with the built-up density, which indicates those areas (wards) have high built-up density and become a less vegetation cover. The high density of vegetation cover (0.74/km²) has been found in ward number 1, 2, 3, 21 and 7 (Fig. 5).

5.4. Variation of LST

The resultant LST variation reveals that the highest temperature (36.99 °C) found in ward number 17 and lowest (32.31 °C) in ward number 2 during the summer season in Contai municipality area. In the ward 9, 13, 14, 15, 16, 17, 18, and 19 temperature is higher than the ward number 1, 2, 3, 4, 5, 6, 7 and 20 (Fig 6a).

As a whole, similar result is found during the winter season. But temperature is high in winter in some additional wards like 1, 2, 3, 4, 6, 12, and 20. Those wards that are warmer in summer become the same in

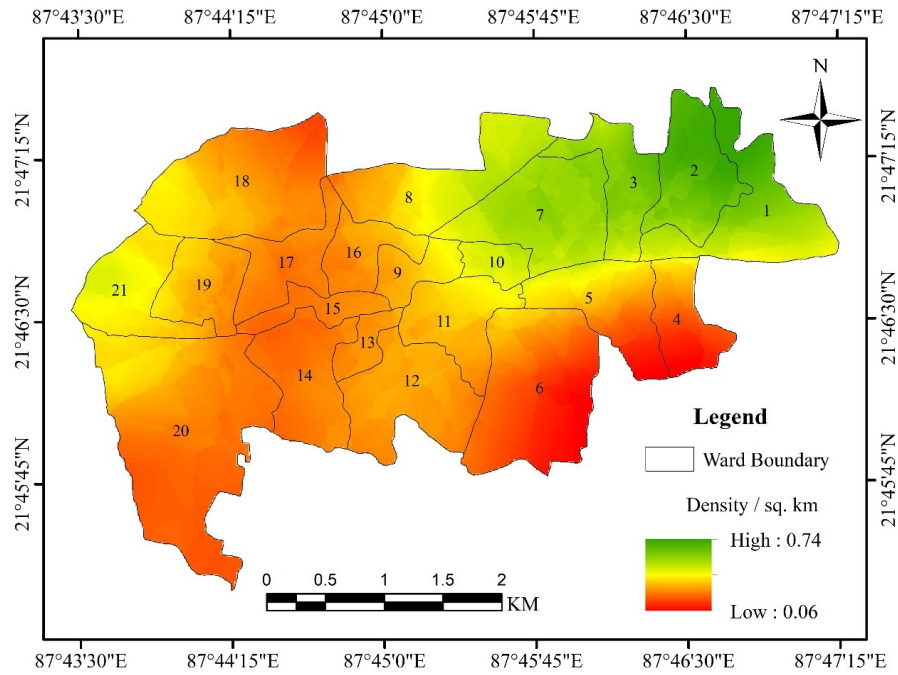Fig. 4 : Variation of built-up density in the Contai municipality area.

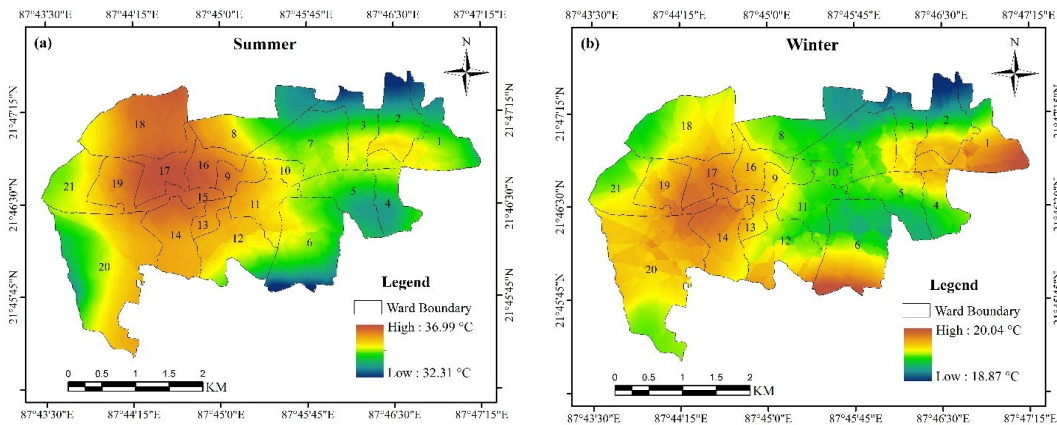Fig. 5 : Density of vegetation covers of Contai municipality area.

Fig. 6 : Temperature distribution during the summer (a) and winter (b) seasons in Contai municipality area.

winter (Fig 6b). Only the highest temperature decreases in the winter season from 36.99 °C to 20.04 °C and lowest from 32.31°C to 18.87 °C in comparison to summer season temperature.

5.5. Relation between the density of settlement and vegetation with LST

The correlation between the density of built-up and LST shows a positive trend (0.11) in summer season. The higher LST has resulted in the areas of a higher

density of built-up areas, whereas, it lower in the low-density areas (Fig. 7a). The correlation between the density of vegetation and LST shows a negative trend (-0.13) in summer. The negative correlation indicates with the higher vegetation density the LST becomes lower than the surrounding low vegetation density areas within the Contai municipality area (Fig. 7c). Such type of relation has also resulted in the other studies in the other urban areas of West Bengal (Pal &Ziaul, 2017; Choudhury et al., 2019; Dhar et al., 2019;

Hoque&Lepcha, 2019) and many other areas around the world (Armson et al., 2012; Santamouris, 2013). Moreover, the relation between the density of built-up and LST shows a mildly negative trend (-0.03) in summer season (Fig. 7b) and the density of vegetation and LST shows positive trend (0.09) in winter season(Fig. 7d) (Sun &Kafatos 2007;Guha &Govil, 2020).

for a significant level of increase of the vegetation cover area. Moreover, the rooftop areas have also been utilized for gardening, which may be the way to minimize the excessive LST. The urban planning is needed to be strictly implemented in the municipal areas for further construction of new settlements. There must be an estimated ratio between the built-up areas
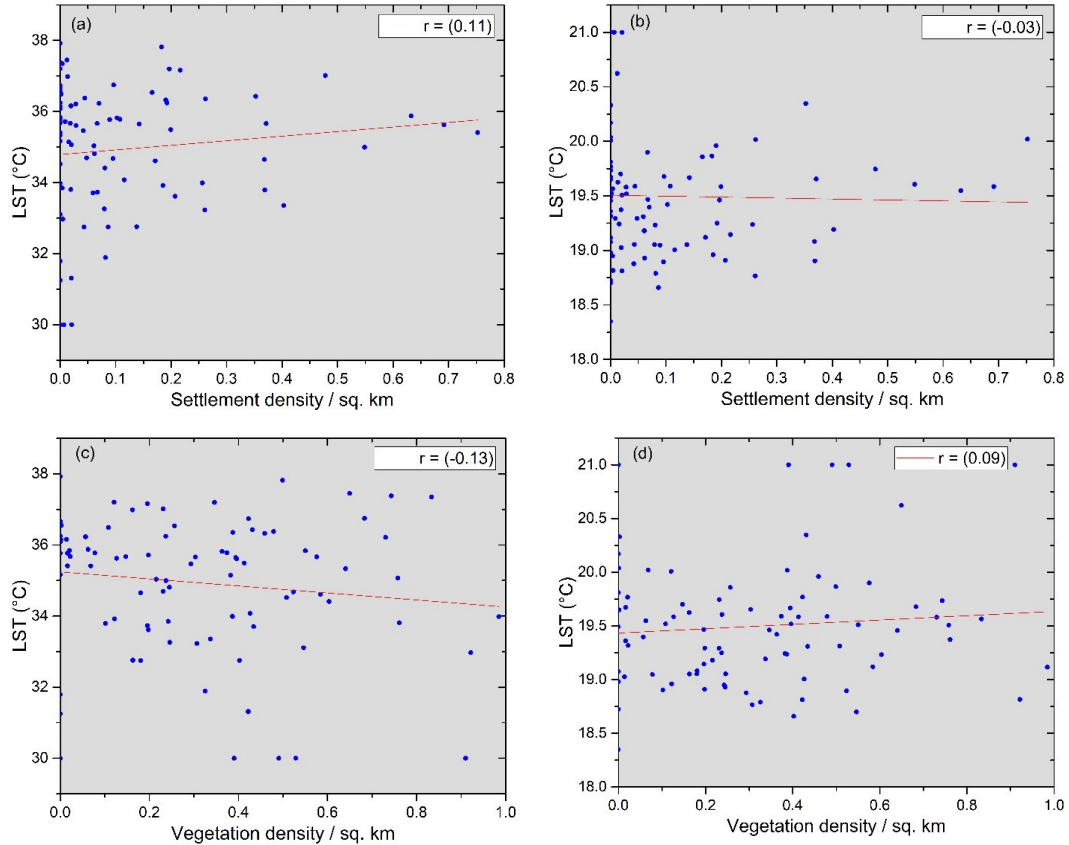

Fig. 7 : The relationship between the density of settlement (a) and (b);density of vegetation (c) and (d) with LST.

6. Conclusion

At present, the heat distribution concept in an urban area is a big issue. Several factors are responsible for that spatio-temporal variation of LST, among those, the LULC pattern is one of the most important of them. Green cover and built-up areas are major responding factors to LST. The present study analyses this concept in the Contai municipality area. The present study reveals the highly-dense built-up areas have recorded the highest LST, which is lowest in the high density of vegetation cover areas in summer season. In recent time, the vacant areas of the dune have been afforested through a social forestry programme which responsible

and vegetation cover areas of the coastal municipality town of Contai, as many hazards of the coastal belt and the sandy tract of urban set up will create more trouble in the near future to stabilise the increase rate of LST.

Conflict of interest

On behalf of all authors, the corresponding author states that there is no conflict of interest.

Acknowledgement

GIS, Vidyasagar University, Midnapore, West Bengal and Apurba Mondal, Research Scholar, Department of Geography, Vidyasagar University, Midnapore,West Bengal for their helpin this research work.

References:

Adelekan, I. O. (2010). Vulnerability of poor urban coastal communities to flooding in Lagos, Nigeria. *Environment and urbanization*, *22*(2), 433-450.

Ahmed, A. Q., Ossen, D. R., Jamei, E., Manaf, N. A., Said, I., & Ahmad, M. H. (2015). Urban surface temperature behaviour and heat island effect in a tropical planned city. *Theoretical and applied climatology*, *119*(3-4), 493-514.

Armson, D., Stringer, P., &Ennos, A. R. (2012). The effect of tree shade and grass on surface and globe temperatures in an urban area. *Urban Forestry & Urban Greening*, *11*(3), 245-255.

Baechler, G. (1998). Why environmental transformation causes violence: A synthesis. *Environmental change and security project report*, *4*(1), 24-44.

Barbier, E. B. (2015). *Climate change impacts on rural poverty in low-elevation coastal zones*. The World Bank.

Bouaziz, M., Eisold, S., &Guermazi, E. (2017). Semiautomatic approach for land cover classification: a remote sensing study for arid climate in southeastern Tunisia. *Euro-Mediterranean Journal for Environmental Integration*, *2*(1), 24.

Chander, G., Markham, B. L., &Helder, D. L. (2009). Summary of current radiometric calibration coefficients for Landsat MSS, TM, ETM+, and EO-1 ALI sensors. *Remote sensing of environment*, *113*(5), 893-903.

Choudhury, D., Das, K., & Das, A. (2019). Assessment of land use land cover changes and its impact on variations of land surface temperature in Asansol-Durgapur Development Region. *The Egyptian Journal of Remote Sensing and Space Science*, *22*(2), 203-218.

Chudnovsky, A., Ben-Dor, E., &Saaroni, H. (2004). Diurnal thermal behavior of selected urban objects using remote sensing measurements. *Energy and buildings*, *36*(11), 1063-1074.

Das, M. K., Bera, M. K., &Chatterji, S. (2013). Management of Water Resources in Urban context of Contai Municipality using Geoinformatics, West Bengal, India. *International Multidisciplinary e-Journal, 2*(2), 7-16.

Das, M., & Das, A. (2020). Assessing the relationship between local climatic zones (LCZs) and land surface temperature (LST)–A case study of Sriniketan-Santiniketan Planning Area (SSPA), West Bengal, India. *Urban Climate*, *32*, 100591.

De Sherbinin, A., Schiller, A., & Pulsipher, A. (2007). The vulnerability of global cities to climate hazards. *Environment and urbanization*, *19*(1), 39-64.

Deng, J. S., Wang, K., Deng, Y. H., & Qi, G. J. (2008). PCA-based land-use change detection and analysis using multitemporal and multisensor satellite data. *International Journal of Remote Sensing*, *29*(16), 4823-4838.

DESA, (2012). *World Urbanization Prospects: The 2011 Revision*, Department of Economic and Social Affairs (Population Division), United Nations, New York.

Dhar, R. B., Chakraborty, S., Chattopadhyay, R., &Sikdar, P. K. (2019). Impact of land-use/land-cover change on land surface temperature using satellite data: A Case study of Rajarhat Block, North 24-Parganas District, West Bengal. *Journal of the Indian Society of Remote Sensing*, *47*(2), 331-348.

Emmanuel, R. (2005). Thermal comfort implications of urbanization in a warm-humid city: the Colombo Metropolitan Region (CMR), Sri Lanka. Building and Environment, 40(12), 1591-1601.

ENVI, A. C. M. (2009). QUAC and FLAASH User's Guide. *Atmospheric Correction Module Version 4.7, Boulder, CO: ITT Visual Information Solutions*.

Farina, A. (2012). Exploring the relationship between land surface temperature and vegetation abundance for urban heat island mitigation in Seville, Spain. *LUMA-GIS Thesis*.

Gartland, L. M. (2012). *Heat islands: understanding and mitigating heat in urban areas*. Routledge.

Grover, A., & Singh, R. B. (2015). Analysis of urban heat island (UHI) in relation to normalized difference vegetation index (NDVI): A comparative study of Delhi and Mumbai. *Environments*, *2*(2), 125-138.

Guha, S., Govil, H., &Besoya, M. (2020). An investigation on seasonal variability between LST and NDWI in an urban environment using Landsat satellite data. Geomatics, Natural Hazards and Risk, 11(1), 1319-1345.

Hokao, K., Phonekeo, V., &Srivanit, M. (2012). Assessing the impact of urbanization on urban thermal environment: A case study of Bangkok Metropolitan. *International Journal of Applied*, *2*(7).

Hoque, I., &Lepcha, S. K. (2019). A geospatial analysis of land use dynamics and its impact on land surface temperature in Siliguri Jalpaiguri development region, West Bengal. *Applied Geomatics*, 1-16.

Jana, S., & Paul, A. K. (2018). Genetical classification of deltaic and non deltaic sequences of landforms of Subarnarekha middle course and lower course sections in Odisha and parts of West Bengal with application of geospatial technology. *Journal of Coastal Sciences, 5*(1), 16-26.

Kantzioura, A., Kosmopoulos, P., &Zoras, S. (2012). Urban surface temperature and microclimate measurements in Thessaloniki. *Energy and buildings*, *44*, 63-72.

Kikon, N., Singh, P., Singh, S. K., & Vyas, A. (2016). Assessment of urban heat islands (UHI) of Noida City, India using multi-temporal satellite data. *Sustainable Cities and Society*, *22*, 19-28.

Lambin, E. F., &Meyfroidt, P. (2011). Global land use change, economic globalization, and the looming land scarcity. *Proceedings of the National Academy of Sciences*, *108*(9), 3465-3472.

Li, X., &Yeh, A. G. O. (2004). Analyzing spatial restructuring of land use patterns in a fast growing region using remote sensing and GIS. *Landscape and Urban planning*, *69*(4), 335-354.

Markham, B., Barsi, J., Kvaran, G., Ong, L., Kaita, E., Biggar, S., ...&Helder, D. (2014). Landsat-8 operational land imager radiometric calibration and stability. *Remote Sensing*, *6*(12), 12275-12308.

McGranahan, G., Balk, D., & Anderson, B. (2007). The rising tide: assessing the risks of climate change and human settlements in low elevation coastal zones. *Environment and urbanization*, *19*(1), 17-37.

Mishra, N., Haque, M. O., Leigh, L., Aaron, D., Helder, D., & Markham, B. (2014). Radiometric cross calibration of Landsat 8 operational land imager (OLI) and Landsat 7 enhanced thematic mapper plus (ETM+). *Remote sensing*, *6*(12), 12619-12638.

Mohan, M., Kikegawa, Y., Gurjar, B. R., Bhati, S., Kandya, A., & Ogawa, K. (2012). Urban heat island assessment for a tropical urban airshed in India.

Moran, M. S., Jackson, R. D., Slater, P. N., &Teillet, P. M. (1992). Evaluation of simplified procedures for retrieval of land surface reflectance factors from satellite sensor output. *Remote Sensing of Environment*, *41*(2-3), 169-184.

NASA. (2016). Landsat 7 Science Data Users Handbook. National Aeronautics and Space Administration, March 19, 2016. https://landsat.gsfc.nasa.gov/wp-content/uploads/2016/08/Landsat7_Handbook.pdf; Retrieved on: 10.12.2019.

Naveh, Z., & Lieberman, A. S. (2013). *Landscape ecology: theory and application*. Springer Science & Business Media.

Nordstrom, K. F. (2004). *Beaches and dunes of developed coasts*. Cambridge University Press.

Oke, T. R. (2002). *Boundary layer climates*. Routledge.

Pal, M., & Mather, P. M. (2004). Assessment of the effectiveness of support vector machines for hyperspectral data. *Future generation computer systems*, *20*(7), 1215-1225.

Pal, M., & Mather, P. M. (2005). Support vector machines for classification in remote sensing. *International journal of remote sensing*, *26*(5), 1007-1011.

Pal, S., & Ziaul, S. K. (2017). Detection of land use and land cover change and land surface temperature in English Bazar urban centre. *The Egyptian Journal of Remote Sensing and Space Science*, *20*(1), 125-145.

Paul, A. K. (2002). *Coastal Geomorphology and Environment: Sundarban Coastal Plain, Kanthi Coastal Plain, Subarnarekha Delta Plain*. ACB publications.

Prado, R. T. A., & Ferreira, F. L. (2005). Measurement of albedo and analysis of its influence the surface temperature of building roof materials. *Energy and Buildings*, *37*(4), 295-300.

Rajeshwari, A., & Mani, N. D. (2014). Estimation of land surface temperature of Dindigul district using Landsat 8 data. *International Journal of Research in Engineering and Technology*, *3*(5), 122-126.

Raleigh, C., &Urdal, H. (2007). Climate change, environmental degradation and armed conflict. *Political geography*, *26*(6), 674-694.

Sahana, M., Dutta, S., & Sajjad, H. (2019). Assessing land transformation and its relation with land surface temperature in Mumbai city, India using geospatial techniques. *International Journal of Urban Sciences*, *23*(2), 205-225.

Santamouris, M. (2007). *Heat island research in Europe: the state of the art*. Advances in Building Energy Research, 1(1), 123–150.

Santamouris, M. (2013). *Environmental design of urban buildings: an integrated approach*. Taylor & Francis, London.

Shi, Y., Sun, X., Zhu, X., Li, Y., & Mei, L. (2012). Characterizing growth types and analyzing growth density distribution in response to urban growth patterns in peri-urban areas of Lianyungang City. *Landscape and urban planning*, *105*(4), 425-433.

Singh, O. P., Khan, T. M. A., & Rahman, M. S. (2001). Has the frequency of intense tropical cyclones increased in the north Indian Ocean?. *Current Science*, 575-580.

Smits, P. C., Dellepiane, S. G., &Schowengerdt, R. A. (1999). Quality assessment of image classification algorithms for land-cover mapping: a review and a proposal for a cost-based approach. *International journal of remote sensing*, *20*(8), 1461-1486.

Sun, D., &Kafatos, M. (2007). Note on the NDVI-LST relationship and the use of temperature-related drought indices over North America. Geophysical Research Letters, 34(24).

Taha, H. (1997). Urban climates and heat islands; albedo, evapotranspiration, and anthropogenic heat. *Energy and buildings*, *25*(2), 99-103.

Wang, F., Qin, Z., Song, C., Tu, L., Karnieli, A., & Zhao, S. (2015). An improved mono-window algorithm for land surface temperature retrieval from Landsat 8 thermal infrared sensor data. *Remote sensing*, *7*(4), 4268-4289.

Wang, J., Huang, B., Fu, D., Atkinson, P. M., & Zhang, X. (2016). Response of urban heat island to future urban expansion over the Beijing–Tianjin–Hebei metropolitan area. *Applied Geography*, *70*, 26-36.

Wu, B., & Ci, L. J. (2002). Landscape change and desertification development in the Mu Us Sandland, Northern China. *Journal of Arid Environments*, *50*(3), 429-444.

Yang, L., & Li, Y. (2009). City ventilation of Hong Kong at no-wind conditions. *Atmospheric Environment*, *43*(19), 3111-3121.

Yuan, F., & Bauer, M. E. (2007). Comparison of impervious surface area and normalized difference vegetation index as indicators of surface urban heat island effects in Landsat imagery. *Remote Sensing of environment*, *106*(3), 375-386.

Ziaul, S., & Pal, S. (2018). Analyzing control of respiratory particulate matter on Land Surface Temperature in local climatic zones of English Bazar Municipality and Surroundings. *Urban climate*, *24*, 34-50.

Ziaul, S., & Pal, S. (2020). Modeling the effects ofgreen alternative on Heat Island Mitigationof a Meso level Town, West Bengal, India. *Advances in Space Research*, *65*(7), 1789-1802.